

MAPPING VENTRICULAR CHANGES RELATED TO DEMENTIA AND MILD COGNITIVE IMPAIRMENT IN A LARGE COMMUNITY-BASED COHORT

Owen T. Carmichael¹, Paul M. Thompson⁷, Rebecca A. Dutton⁷, Allen Lu⁷, Sharon E. Lee⁷, Jessica Y. Lee⁷, Lewis H. Kuller², Oscar L. Lopez³, Howard J. Aizenstein⁵, Carolyn Cidis Meltzer^{3,5,8,9,10}, Yanxi Liu^{6,11}, Arthur W. Toga⁷, James T. Becker^{3,4,5}

Department of Neurology, University of California, Davis¹; Departments of Epidemiology², Neurology³, Psychology⁴, Psychiatry⁵, and Radiology⁶, University of Pittsburgh; Department of Neurology, University of California, Los Angeles⁷; Departments of Radiology⁸, Neurology⁹ and Psychiatry¹⁰, Emory University; The Robotics Institute, Carnegie Mellon University¹¹

ABSTRACT

We present a fully-automated technique for visualizing localized cerebral ventricle shape differences between large clinical subject groups who have received a magnetic resonance (MR) image scan. The technique combines a robust, automated technique for ventricular segmentation with a 3D surface-based radial thickness mapping approach that allows spatially-localized statistical tests of relative shape differences between clinical groups. The technique is used to analyze localized ventricular expansion in Alzheimer's Disease (AD) and mild cognitive impairment (MCI) in a large cohort of community-dwelling elderly individuals (N=339). The resulting maps are the first to chart localized ventricular dilation in a cohort of this size. Besides showing patterns of ventricular expansion that may be consistent with the spatial progression of AD-related pathology, the maps reveal new information about localized ventricular atrophy that may have been overlooked to date. A detailed understanding of spatial atrophy patterns may be useful for early disease detection or for patient monitoring in drug trials.

1. INTRODUCTION

A growing body of studies have associated accelerated dilation of the cerebral ventricles with risk for and progression of dementia and MCI in elderly subjects [1] [3] [5]. Therefore, ventricular volume measurements from structural MR or computed tomography (CT) images have been proposed as a possible biomarker for estimating dementia risk or response to treatments. However, two important methodological issues have limited the large-scale applicability of previous studies that related ventricular expansion with dementia progression.

First, most previous studies relied on manual or semi-automated assessments of ventricular size through which a human operator views each image in the study and assigns

them qualitative ventricular size ratings or marks anatomical boundaries. Due to the expense and time required to train human operators to consistently rate images, typical studies involve a small number of subjects (*e.g.*, 30-50), to the detriment of statistical power.

Second, previous studies have summarized relative ventricular expansion between groups in terms of overall volume or qualitative measures of atrophy. While overall ventricular volume can be a useful proxy measure for overall neuronal death in periventricular structures, it does not provide anatomically-specific information about which structures may be experiencing the deficits that are reflected in ventricular expansion. Maps of regional patterns of ventricular expansion in dementia and MCI may lead to greater insight into the progression of underlying pathological processes and more specific biomarkers for disease progression and risk.

In this study, we present a technique for fully-automated 3D mapping of regional differences in ventricular volume between large groups of normal subjects, subjects with AD, and subjects with MCI. We use a fully-automated, reliable technique for MR-based lateral ventricle segmentation to alleviate human operator issues [6] [7], and we use a 3D surface-mesh based spatial mapping technique to explore regional differences between the ventricles of AD, MCI, and control subjects [8] [5]. In so doing, we extend earlier results on regional mapping of ventricular differences between smaller groups of AD and control subjects [5]. We also expected that spatial maps of ventricular differences would reveal anatomically-specific information about the dementia process, as it has for other diseases [9].

2. METHODS

Subjects. There were 388 subjects who received clinical evaluations and high-resolution MR scans in 1997-99 as part of the Cardiovascular Health Study (CHS) Cognition Study at the Pittsburgh center. Subjects were categorized as cognitively normal or diagnosed with MCI or AD using diagnostic

This work was supported by NIH grants NS07391, MH064625, AG05133, DA015900-01, MH01077, EB001561, RR019771, RR021813, AG016570, NIA-R01-20098.

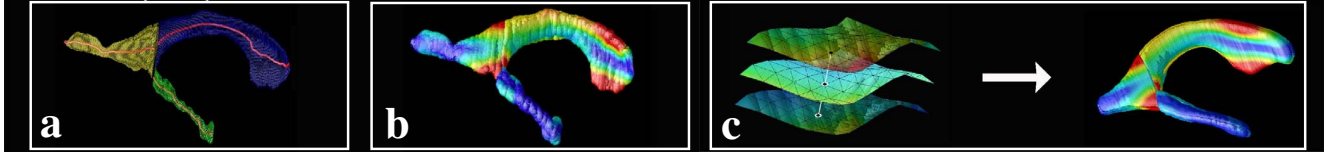


Fig. 1. Construction of Ventricular Maps. 1a. Medial curves (red) are extracted from mesh representations of the frontal, posterior, and temporal horns of the lateral ventricles (blue, yellow, and green respectively). 1b. The radial distance of each ventricular boundary point to a medial curve can be interpreted as a local thickness measure at that boundary point. Here, boundary points are color mapped by distance to the medial curve, with blue (red) points being closer to (farther from) the medial curve. 1c. Maps of boundary-to-medial-curve distances are averaged across all subjects in a group. Group average maps can then be compared between groups as in Figure 2.

criteria and clinical procedures reported previously [10] [11]. Subjects diagnosed with Non-AD dementias ($N=6$) were excluded from analysis due to their rarity and high variability in clinical features. A complete clinical evaluation and high-quality imaging data was available for 339 subjects. Age mean and standard deviation overall and in the normal, MCI, and AD groups were 73.6 and 4.2, 72.6 and 3.4, 74.5 and 4.4, and 77.9 and 5.2. The number of male and female subjects overall, and in normal, MCI, and AD groups were 208 and 131, 135 and 90, 46 and 28, and 27 and 13. All MR images were collected using a single 1.5T Signa scanner (GE Medical Systems) with high performance gradients (4 G/cm and 150 T/m-s). The subjects were positioned in a standard head coil and a volumetric Spoiled Gradient Recalled (SPGR) acquisition sequence with parameters optimized for maximal contrast among gray matter, white matter, and cerebrospinal fluid was acquired in the coronal plane (TE/TR = 5/25, flip angle = 40 deg., NEX = 1, slice thickness = 1.5mm/0mm interslice).

Fully-Automated Lateral Ventricle Segmentation Lateral ventricular volumes were estimated fully automatically on all scans using a technique described in a previous study and validated on a set of dilated ventricles [6] [7]. Images were resampled to obtain $1 \times 1 \times 1 \text{ mm}^3$ voxels, anisotropically smoothed [12], skull-stripped [13], cropped to remove all-zero planes, and nonlinearly aligned [14] to a reference image on which the lateral ventricles had been traced by an trained rater. The nonlinear alignment technique first used Levenberg-Marquardt optimization to estimate rigid-body and piecewise-linear transformations between subject and reference images, using a sum-of-squared-distances (SSD) cost function. Then, a dense voxel-by-voxel refinement of the piecewise-linear transformation was computed using gradient descent optimization. The reference image was a randomly-selected MR image of a control subject from a previous study. We note that prior validation experiments suggest that ventricular segmentation accuracy does not depend on high similarity between the subject and reference images [7]. The lateral ventricles were delineated on the reference image to include the frontal horn and body, as well as the temporal and poste-

rior horns, using a tracing protocol described previously [15]. The alignment between subject and reference images allowed the ventricle tracing to be transferred from the reference image to the subject image. Automated ventricular tracings estimated in this way were converted into uniformly parameterized 3D surface meshes as in [15] for subsequent shape and thickness analysis.

Ventricular Shape and Radial Thickness Mapping. 3D central curves were derived from the surface meshes by threading down the center of each of the three ventricular horns (see Figure 1; see also [8] [5]). Distance maps were computed indexing local expansion of the ventricular boundary from the medial curves in each subject. These surface-to-core radial distance fields were then averaged at corresponding surface locations across subjects, and compared statistically between groups, at equivalent ventricular surface points in 3D space.

Ventricular Statistical Maps. For all possible contrasts between pairs of dementia status groups (AD, MCI, and normal), statistical maps were generated indicating local group differences in radial ventricular expansion. A multiple regression was run to assess whether the ventricular expansion at each surface point depended on dementia status. The p value describing the significance of this linkage was plotted onto the surface at each point producing a color-coded statistical map (see Figure 2 for examples). These maps reveal where diagnosis is associated with regional ventricular dilation. Overall p values were assigned to the maps by permutation testing. As in [5], the total area of the surface with statistics exceeding a predefined fixed threshold (here $p = 0.01$) was assessed and compared with the null distribution assembled by permuting the group assignments.

3. RESULTS

Spatial maps of mean radial distance, percent differences in radial distance maps between groups and maps of p values for group differences are shown in Figure 2. Pronounced deficits are seen in MCI subjects relative to normal subjects at the posterior end of the superior-medial boundary of the frontal horns, and extending along the diverging occipital horns (row

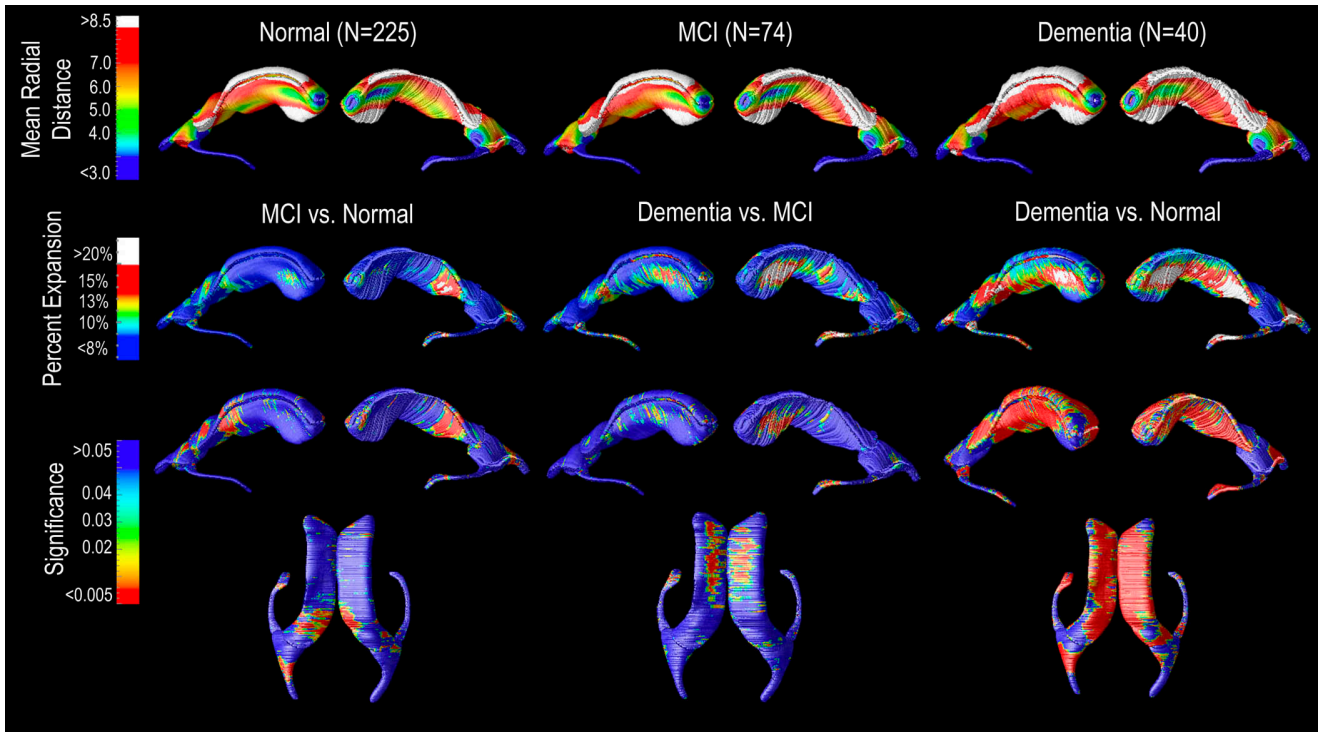


Fig. 2. Maps of Ventricular Expansion. A measure of radial distance is averaged across patients and, separately, across controls, and plotted on group average ventricular shapes. Red colors in the diseased group (a) indicate frontal horn expansions, relative to healthy controls. (b) plots the ratio of the mean radial size in disease versus controls, revealing regions with severe expansion radially (red colors). (c) shows the significance of these changes at each surface point. Changes in all three components are highly significant, even when corrected for multiple comparisons using permutation testing.

4, column 1). Deficits (*i.e.*, relative expansions) are also seen in MCI subjects along the lateral boundaries of the frontal horns near their posterior limit, the anterior tip of the left temporal horn, and the posterior limit of the left occipital horn (row 3, column 1). In contrast, deficits in demented subjects relative to MCI subjects are pronounced along the more anterior portions of the superior-medial boundary of the frontal horns (row 4, column 2), and along the lateral boundaries of the frontal horns near their anterior limit (row 4, column 3). The deficit at the tip of the left temporal horn is more pronounced between demented subjects and MCI subjects than between MCI subjects and normal subjects. Contrasts between normal and demented subjects show dramatic ventricular atrophy throughout the lateral ventricles, especially along the frontal and temporal horns. Mean ventricular volume was 113% higher in MCI subjects compared to normal subjects, and mean volume was 119% higher in AD subjects compared to MCI subjects. The difference in mean volume was significant between normals and MCI subjects at the $p = .05$ level, and between MCI and AD subjects the difference showed a strong trend toward significance (two-tailed t tests, $p = .038$ and $p = .053$).

4. DISCUSSION

Since MCI is often a transitional state between normal cognitive function and AD, a spatial progression of ventricular changes from normal cognitive function through MCI to AD can be inferred from the statistical maps, even though the maps are based on cross-sectional comparisons between groups. The maps depict two patterns of ventricular dilation that may be consistent with earlier histopathological studies of the spatial progression of AD-related pathologies. Specifically, the apparent posterior-to-anterior progression of ventricular expansion along the superior-medial boundary may be related to the posterior-to-anterior progression of amyloid plaques in the nearby cingulate cortex that (partially) characterizes early AD pathology [16]. The other characteristic pathological feature in AD, the progression of neurofibrillary tangles from the medial temporal lobe outwards, may be reflected in the statistical maps through the progressive expansion of the tips of the temporal horn, which border medial temporal lobe structures. Furthermore, localized ventricular expansion along the lateral and occipital boundaries may reflect damage to periventricular white matter tracts or other structures.

Statistical analysis of the spatial progression of ventricu-

lar dilation through transitions from normal cognitive function to MCI and AD was made possible by the radial thickness mapping technique described above, which enabled tests of relative expansion between groups at localized points on a 3D surface. We believe that radial thickness mapping may provide localized shape information that is complementary to that provided by other shape mapping techniques based on alternative surface representations [17] [18], medial shape descriptors [19][20], or combinations of both [21].

Analysis of a large number of subjects was made possible by the automated ventricular segmentation technique, which obviated the need for time-consuming and possibly unreliable manual interaction with each image. In the future, we hope that the automated technique will be augmented to reliably segment a wider variety of brain structures and automatically assess uncertainty in structure boundaries.

5. REFERENCES

- [1] L. H. Kuller, O. L. Lopez, A. Newman, N. J. Beauchamp, G. Burke, C. Dulberg, A. Fitzpatrick, L. Fried, and M. N. Haan, "Risk factors for dementia in the cardiovascular health cognition study," *Neuroepidemiology*, vol. 22, no. 1, pp. 13–22, January 2003.
- [2] N.D. Prins, E.J. van Dijk, T. den Heijer, S.E. Vermeer, P.J. Koudstaal, M. Oudkerk, A. Hofman, and M.M. Breteler, "Cerebral white matter lesions and the risk of dementia," *Arch Neurol*, vol. 61, no. 10, pp. 1503–1504, October 2004.
- [3] C. DeCarli, J.V. Haxby, J.A. Gillette, D. Teichberg, S.I. Rapoport, and M.B. Schapiro, "Longitudinal changes in lateral ventricular volume in patients with dementia of the Alzheimer type," *Neurology*, vol. 42, pp. 2029–2036, October 1992.
- [4] J.S. Luxenberg, J.V. Haxby, H. Creasey, M. Sundaram, and S.I. Rapoport, "Rate of ventricular enlargement in dementia of the Alzheimer type correlates with rate of neuropsychological deterioration," *Neurology*, vol. 37, pp. 1135–1140, July 1987.
- [5] P.M. Thompson, K.M. Hayashi, G. de Zubicaray, A.L. Janke, S.E. Rose, J. Semple, M.S. Hong, D. Herman, D. Gravano, D.M. Doddrell, and A.W. Toga, "Mapping hippocampal and ventricular change in Alzheimer's disease," *NeuroImage*, vol. 22, no. 4, pp. 1754–1766, August 2004.
- [6] O. T. Carmichael, H. A. Aizenstein, S. W. Davis, J. T. Becker, P. M. Thompson, C. C. Meltzer, and Y. Liu, "Atlas-based hippocampus segmentation in Alzheimer's disease and mild cognitive impairment," *NeuroImage*, vol. 27, no. 4, pp. 979–990, October 2005.
- [7] O. T. Carmichael, P. M. Thompson, R. A. Dutton, A. Lu, S. E. Lee, J. Y. Lee, H. J. Aizenstein, Y. Liu, O. L. Lopez, C. C. Meltzer, A. W. Toga, and J. T. Becker, "Fully-automated segmentation of lateral ventricles in aids patients," Under editorial review, *Journal of Magnetic Resonance Imaging*, 2005.
- [8] P.M. Thompson, C. Schwartz, and A.W. Toga, "High-resolution random mesh algorithms for creating a probabilistic 3d surface atlas of the human brain," *NeuroImage*, vol. 3, no. 1, pp. 19–34, March 1996.
- [9] M. Styner, J.A. Lieberman, R.K. McClure, D.R. Weinberger, D.W. Jones, and G. Gerig, "Morphometric analysis of lateral ventricles in schizophrenia and healthy controls regarding genetic and disease-specific factors," *Proc Nat Acad Sci*, vol. 102, no. 13, pp. 4872–7, March 2005.
- [10] O. L. Lopez, L. H. Kuller, A. Fitzpatrick, D. Ives, J. T. Becker, and N. Beauchamp, "Evaluation of dementia in the cardiovascular health cognition study," *Neuroepidemiology*, vol. 22, no. 1, pp. 1–12, January 2003.
- [11] O.L. Lopez, W.J. Jagust, S.T. DeKosky J.T. Becker, A. Fitzpatrick, C. Dulberg, J. Breitner, C. Lyketsos, B. Jones, C. Kawas, M. Carlson, and L.H. Kuller, "Prevalence and classification of mild cognitive impairment in the cardiovascular health study cognition study: Part 1," *Arch Neurol*, vol. 60, no. 10, pp. 1385–1389, October 2003.
- [12] S.M. Smith and J.M. Brady., "SUSAN - a new approach to low level image processing," *IJCV*, vol. 23, no. 1, pp. 45–78, May 1997.
- [13] S. Smith, "Fast robust automated brain extraction," *Human Brain Mapping*, vol. 17, no. 3, pp. 143–155, 2002.
- [14] M. Chen, *3-D Deformable Registration Using a Statistical Atlas with Applications in Medicine*, Ph.D. thesis, Robotics Institute, Carnegie Mellon University, Pittsburgh, PA, October 1999.
- [15] K. L. Narr, P. M. Thompson, T. Sharma, J. Moussai, R. Blanton, B. Anvar, A. Edris, R. Krupp, J. Rayman, M. Khaledy, and A. W. Toga, "Three-dimensional mapping of temporolimbic regions and the lateral ventricles in schizophrenia: Gender effects," *Biol. Psychiatry*, vol. 50, pp. 84–97, 2001.
- [16] H. Braak and E. Braak, "Neuropathological staging of Alzheimer-related changes," *Acta Neuropathol*, vol. 82, pp. 239–259, 1991.
- [17] A. Kelemen, G. Szekely, and G. Gerig, "Elastic model-based segmentation of 3-d neuroradiological data sets.," *IEEE Trans. Med. Imaging*, vol. 18, no. 10, pp. 828–839, October 1999.
- [18] J.G. Csernansky, L. Wang, S. Joshi, J.P. Miller, M. Gado, D. Kido, D. McKeel, J.C. Morris, and M.I. Miller, "Early DAT is distinguished from aging by high-dimensional mapping of the hippocampus," *Neurology*, vol. 55, no. 11, pp. 1636–1643, 2000.
- [19] SM Pizer, DS Fritsch, P Yushkevich, V Johnson, E Chaney, and G Gerig, "Segmentation, registration, and measurement of shape variation via image object shape," *IEEE Trans. Med. Imaging*, vol. 18, no. 10, pp. 851–865, October 1999.
- [20] P.T. Fletcher, C. Lu, S.M. Pizer, and S. Joshi, "Principal geodesic analysis for the study of nonlinear statistics of shape," *IEEE Trans. Med. Imaging*, vol. 23, no. 8, pp. 995–1005, August 2004.
- [21] M. Styner, J.A. Lieberman, D. Pantazis, and G. Gerig, "Boundary and medial shape analysis of the hippocampus in schizophrenia," *Med. Img. Anal.*, vol. 8, no. 3, pp. 197–203, September 2004.